J Mater Sci: Mater Med (2011) 22:357–369
DOI 10.1007/s10856-010-4214-2

Magnetically mediated release of ciprofloxacin from polyvinyl alcohol based superparamagnetic nanocomposites

A. K. Bajpai · Rashmi Gupta

Received: 29 August 2010 / Accepted: 9 December 2010 / Published online: 29 December 2010

Abstract Polymer nanocomposites exhibiting superparamagnetic behavior have been recognized as a promising tool to achieve targeted drug delivery using external magnetic field for treating complex diseases like cancers and tumors. The present investigation attempts to design a superparamagnetic nanocomposite which could desirably deliver ciprofloxacin drug by application of varying magnetic field. In order to achieve the proposed objectives, a polymer matrix of polyvinyl alcohol-g-polymethyl methacrylate was prepared by free radical polymerization and iron oxide particles were impregnated by in situ precipitation method. The prepared nanocomposites were characterized by techniques like FTIR, electron microscopy (SEM and TEM) and XRD and magnetization studies were performed to ensure superparamagnetic behavior. The antibiotic drug ciprofloxacin was loaded onto the magnetic nanocomposites and the influence of various factors such as percent loading, chemical composition of the nanocomposite, applied magnetic field, pH of the release medium were investigated on the release profiles of the drug. The chemical integrity of the drug and its antibacterial potential were also studied. The dynamics of the release process was also examined mechanistically.

1 Introduction

Magnetic materials have been proposed for biomedical purposes to a large extent for several years [1]. Recently, controlling the rate and period of drug delivery as well as targeting specific locations of the body for treatment has become popular. Therefore, the goal of the drug delivery systems is to put the medications to particular parts of the body by means of either a physiological or a chemical trigger, such as "smart" drug carriers, as it provides numerous advantages over the conventional routes of drug delivery. Up to now, many stimuli-responsive polymers in response to environmental changes such as temperature, pH, external magnetic field (MF) and mechanical signal have been reported [2].

Magnetically controlled drug targeting is one of the various possibilities of drug targeting [3–6]. Recently, magnetic nanoparticles in biomedical applications have become increasingly important, due to the fact that they can be triggered via a non-contact force. Superparamagnetic iron oxide nanoparticles (SPIONs) characterized by higher magnetization and good biocompatibility have attracted significant attention as magnetic drug targeting carriers, enhanced resolution magnetic resonance imaging, tissue repair, cell and tissue targeting and transfection. Superparamagnetism in many biomedical applications such as drug delivery is useful because the SPION can be transported by electrical field effects to the desired site and once the external magnetic field is removed, magnetization disappears and the SPION can remains at the target site for a certain period [7].Two types of iron oxide have mainly been investigated for their use in magnetic nanoparticle formulation: maghemite (γ-Fe_2O_3) and magnetite (Fe_3O_4) due to their high saturation magnetization and high magnetic susceptibility; the magnetite (Fe_3O_4) particles are preferred because of their greater saturation magnetization and biocompatibility make them a more promising candidate for various biomedical applications [8].

A. K. Bajpai (✉) · R. Gupta
Bose Memorial Research Laboratory, Department of Chemistry, Government Autonomous Science College, Jabalpur 482001, MP, India
e-mail: akbmrl@yahoo.co.in; akbajpailab@yahoo.co.in

In this study, a new simple method has been proposed for preparation of magnetic nanocomposite hydrogels that involves in situ synthesis of homogeneously dispersed superparamagnetic nanoparticles within a hydrogel matrix prepared by graft copolymerization of methyl methacrylate (MMA) onto polyvinyl alcohol (PVA). The selection of PVA as one of the components of the hydrogel was due to its unlimited applications in medicine, biology and technology, such as contact lenses, artificial meniscus and reconstruction of vocal cords. Hydrogels of PVA are also known for protein adsorption and cell adhesion [9]. PMMA has also been employed as a popular material for various technological and biomedical applications such as bone cement and targeted drug delivery systems [10]. The drug chosen for the study is ciprofloxacin [1-cyclopropyl-6-fluoro-1, 4-dihydro-4-oxo-7-(1-piperazinyl)-3-quinoline carboxylic acid hydrochloride monohydrate]. Ciprofloxacin (CFx) is a broad-spectrum anti-infective agent of the synthetic antibiotic, belonging to a group called fluoroquinolone. Its mode of action depends upon blocking bacterial DNA replication by binding itself to an enzyme called DNA gyrase, thereby causing double-stranded breaks in the bacterial chromosome [11]. Furthermore, excessive doses of antibiotic drugs can cause severe harmful effects and, therefore, for avoiding administration of overdose a control and targeted delivery could be a better option. This paper outlines the specific studies and processes that were followed to ultimately demonstrate that the nanocomposite hydrogels can be a useful tool in magnetically controlled drug delivery devices.

2 Experimental

2.1 Materials

Polyvinyl alcohol (PVA) (98% hydrolyzed, soluble in hot water at 80°C, mol. wt ca. 14000), was obtained from E. Merck, India, and used without any pretreatment. Monomer, methyl methacrylate (MMA) was obtained from Sigma-Aldrich Co(USA) and washed thrice in 5% NaOH, 5% H_2SO_4 and bidistilled water, respectively and freed from the inhibitor by further distilling it under vacuum. N, N′-methylene bisacrylamide (MBA) (Research Lab Mumbai, India) was used as a crosslinking agent, while potassium persulphate (KPS) (Loba Chemie, India) and potassium metabisulphite (MBS) (Qualigens Fine Chemicals, Mumbai India) were used as an initiator and activator, respectively. The drug Ciprofloxacin (CFx) (Mol.wt. 331.4, soluble in dilute 0.01 N HCl and practically insoluble in water and ethanol) was manufactured by Cipla Ltd., Roorkey, Uttarakhand, India and supplied in the form of injections (2 mg/mL). $FeCl_2{\cdot}4H_2O$ and $FeCl_3{\cdot}6H_2O$ salts were obtained from Merck (India) and used as received. Bidistilled water was used throughout the experiments.

2.2 Methods

2.2.1 Preparation of iron oxide nanoparticles

For synthesis of iron oxide nanoparticles the solution of Fe ions was prepared from $FeCl_2{\cdot}4H_2O$ and $FeCl_3{\cdot}6H_2O$ salts ($Fe^{2+}/Fe^{3+} = 0.5$) in acidic condition (pH 2.19) by continuous stirring the solution for 0.5 h under nitrogen atmosphere and at room temperature as per the modified method reported in literature [12]. A solution of 10% NaOH was added dropwise into the solution of Fe ions to precipitate nanoparticles of iron oxide according to the reaction given below:

$$2FeCl_3 + FeCl_2 + 8NH_4OH \rightarrow Fe_3O_4 + 8NH_4Cl + 4H_2O$$

The precipitated iron oxide nanoparticles were filtered and repeatedly washed with distilled water.

2.2.2 Preparation of grafted hydrogel

The hydrogel was prepared by a redox polymerization method as reported earlier [13]. In brief, known amounts of PVA, purified monomer (MMA) and crosslinker (MBA) were taken in aqueous medium and precalculated amounts of redox system comprising of persulphate and metabisulphite were added into the reaction mixture in one shot to initiate graft copolymerization. The reaction mixture was taken in a rectangular glass mould (8 cm × 10 cm) and kept for 24 h at 35°C so that the whole fluid converted into a semi-transparent thin film.

2.2.3 Purification of hydrogel

The thin films prepared as above were allowed to swell in bidistilled water till equilibrium so that the unreacted chemicals including salts were leached out and the gels become free of any unreacted impurities. The fully swollen gels were dried at room temperature, cut into small rectangular pieces (1 cm × 1 cm) and stored in airtight polyethylene bags.

2.2.4 Swelling experiments

The extent of swelling of grafted hydrogel was determined by a conventional gravimetric procedure as reported in literature [14]. The swelling ratio was determined by the following Eq. (1),

$$\text{Swelling ratio } (S_r) = \frac{\text{Weight of swollen gel}}{\text{Weight of dry gel}} = \frac{W_s}{W_d} \quad (1)$$

The amount of water imbibed by the sample provides information about the hydrophilic nature of the material which is essentially one of the criterions of biocompatibility.

2.2.5 Impregnation of ion oxide into the gel

The dried and purified gels were placed in an aqueous solution of mixture of ferrous (0.5 M) and ferric salts (0.6 M) of known molar ratio (1:1) and allowed to swell for 24 h so that both ferrous and ferric ions were entrapped into the polymer matrices. Prior to putting them in salt solutions a dry stream of N_2 was flushed for at least one hour. The swollen gels were taken out and washed by mildly shaking them in distilled water so that surface of gel was properly washed and freed from unreacted salts and chemicals. The swollen gels were taken out, washed several times with water and dried at room temperature for 72 h. The dried gels were then put into alkaline solution (10% NaOH or NH_4OH) for definite time period so that ferrous and ferric ions get precipitated within the polymer matrix and formation of magnetite is obtained.

The change in color of the gel turns from red to dark red brown also confirms the formation of oxides of iron. The prepared iron oxide-polymer nanocomposites were washed, dried at room temperature for a week and stored in airtight polyethylene bags.

The percentage impregnation of iron oxide was calculated by the following Eq. (2):

$$[\%]\ \text{Impregnation of iron oxide} = \frac{\{W_{\text{impregnated}} - W_{\text{dry}}\}}{W_{\text{dry}}} \times 100 \quad (2)$$

where $W_{\text{impregnated}}$ is the weight of dry impregnated gel and W_{dry} is the initial weight of hydrogel.

2.2.6 Control of particle size

The control of particle size is commonly achieved by the use of capping agents such as surfactants molecules, polymers, organic and/or organometallic ligands, and macrocyclic molecules. They typically interact with the growing metal particles via a mechanism of surface adhesion, ultimately inhibiting the aggregation process. Since the metal nanoclusters formation is sensitive to the presence of polymers during the synthesis process [15], in the present study also the presence of grafted polymer (PVA-g-MMA) tends to maintain the size of the iron oxide nanoparticles and hinders the aggregation process. This obviously ensures a narrow size distribution of nanoparticles and homogenous deposition of nanoparticles within the polymer matrix.

2.2.7 Loading of drug

In a typical loading experiment, known volume of drug (CFx) was diluted with appropriate amount of phosphate buffer saline (PBS) solution and shaken vigorously for mixing of drug and PBS solution. The drug loaded gels were prepared by allowing 0.1 g of gel pieces to swell in freshly prepared drug solution (10 mL) till equilibrium. The following equation was used to calculate the % loading,

$$[\%]\ \text{loading} = \frac{W_d - W_o}{W_o} \times 100 \quad (3)$$

where W_d and W_o are the dry weights of loaded and unloaded nanocomposite pieces, respectively.

3 Characterization

The prepared nanocomposites were characterized by the following methods as discussed below.

3.1 FT-IR

In order to provide an evidence for grafting of PMMA chains onto PVA backbone and impregnation of magnetite into the grafted hydrogel matrix, FTIR spectra of native PVA and iron oxide impregnated hydrogel were recorded from 4000 to 400 cm^{-1} using an FTIR-8400S, Shimadzu spectrophotometer.

3.2 Electron microscopy

The morphological features of the nanocomposites and iron oxide particles were investigated by recording scanning electron micrographs (STEREO SCAN, 430, Lecica, SEM, USA) and transmission electron micrographs (Hitachi Hu-11 B with an accelerating voltage of 200 kV), respectively.

3.3 X-ray diffraction (XRD)

The X-ray diffraction studies of the nanoparticles and nanocomposites were carried out on Rigaku Rotting anode mode Ru-H3R (18 KW), X-ray powder diffractometer. The diffraction data were collected from 10 to 60°, $2°\theta$ values with a step size of 0.02 and counting time of 2 s $step^{-1}$ using wavelength of 1.54 Å. The average crystallite size of iron oxide particles were estimated using Scherer's formula.

3.4 Magnetization studies using VSM

Vibrating sample magnetometer (Oxford, VSM) was used to evaluate magnetic moments of both the prepared iron oxide nanoparticles and nanocomposites at room temperature as a function of the applied magnetic field.

3.5 Biopharmaceutical characterization

3.5.1 Magnetically induced in vitro release experiments

Magnetically induced in vitro release of the encapsulated CFx were carried out by placing the dried and loaded nanocomposites (0.1 g) in a test tube containing a definite volume (10 mL) of PBS (Phosphate Buffer Saline) as the release medium (pH 7.4) and subjected to gently shaking for definite time period (1.25 h) in the absence and presence of the MF (Electromagnet Model EM-07), respectively. The average MF applied to the nanocomposites was 75 G, which was measured by using a Digital Gaussmeter (Model DGM-20). At predetermined time intervals (15 min) 5 mL supernatant was withdrawn from the release medium and replacing it with fresh PBS. The amount of CFx released from the nanocomposite was measured spetrophotometrically at 278 nm (Shimandzu 1700 Phama Spec.) and the amount of CFx released was determined with the help of calibration plot.

3.5.2 Release kinetics

The release of drug from the gels (initially dried) involves the absorption of water into the matrix and simultaneous release of drugs via diffusion, as governed by Fick's law. The process can be modeled using a free volume approach [16] or a swelling–controlled release mechanism. In the present investigation the release device belongs to a swelling controlled type of delivery system which involves three consecutive steps: absorption of water into the polymeric matrix, dissolution of drug into the imbibed water and finally diffusion of the drug into the external release medium. More importantly, the release of drug is basically determined by the process of relaxation of macromolecular chains and the diffusion of the entrapped drug molecules into the exterior medium.

In order to have mechanistic insights into the drug transport processes the kinetic data of the release process were fitted into various equations which are basically derived from the Fick's law.

$$\frac{W_t}{W_\infty} = kt^n \tag{4}$$

where W_t and W_∞ are the amounts of drug released at time t and infinite time (equilibrium amount of drug released), respectively and k is the rate constant. The exponent n, called diffusional exponent is an important indicator of the mechanism of drug transport. For $n > 0.5$, non-Fickian diffusion is observed while $n = 0.5$ represents a Fickian diffusion mechanism. The value of $n = 1$ provides case II transport mechanism in which the drug releasing from a hydrogel of slab geometry will be of zero order. It is notable here that release occurs as soon as the matrix is placed in contact with the fluid. For calculating diffusion constant of the drug the following Fickian diffusion equation can be used:

$$\frac{W_t}{W_\infty} = 4\left[\frac{Dt}{\pi L^2}\right]^{0.5} \tag{5}$$

where D is the diffusion constant of the drug ($cm^2\ s^{-1}$) and l is the thickness of the dry and drug loaded gel. The diffusion constant and values of n calculated for various hydrogel compositions are summarized in Table 1.

Table 1 Data showing the kinetic parameters for the water sorption process

S. no	PVA (g)	MMA (mmol)	MBA (mmol)	Diffusion constant $D \times 10^8$ cm^2/s	*n*	Mechanism
1	1.5	9.35	0.06	15.4	0.65	Anomalous
2	2.0	9.35	0.06	9.6	0.48	Fickian
3	2.5	9.35	0.06	6.9	0.93	Anomalous
4	3.0	9.35	0.06	5.7	0.65	Anomalous
5	2.0	4.67	0.06	7.6	0.33	Fickian
6	2.0	18.69	0.06	10.8	0.67	Anomalous
7	2.0	28.04	0.06	10.5	0.81	Anomalous
8	2.0	9.35	0.00	8.14	0.44	Fickian
9	2.0	9.35	0.19	15.1	0.78	Anomalous
10	2.0	9.35	0.26	16.6	0.62	Anomalous

3.6 Drug activity

3.6.1 UV spectral study

In order to check the chemical integrity of entrapped drug, the UV spectral study (Shimandzu 1700 Pharma Spec) was performed. For this purpose UV spectra of pure CFx solution and released fractions were compared at different time periods.

3.6.2 Antibacterial activity

Antibacterial activity of the loaded hydrogel nanocomposites has been demonstrated by disk diffusion method (Kirby- Bauer) method. The standardization disk diffusion procedure of Bauer et al. [17] has been widely accepted for testing bacterial susceptibility to antimicrobial agents. Briefly, at first nutrient agar plate was prepared by dissolving 2.8 g of nutrient agar (Hi-Media, Mumbai, India) in 100 mL of distilled water, heated to boiling to dissolve the medium completely and then autoclaved in 121°C, 15 lbs for 15 min.

Agar plates were seeded with 50 μL of bacterial culture (*Escherichia coli* {MTCC 1304}) (titer value 10^4 Cfu/mL), and lawn was prepared by spread plate method. The surface of the seeded media was allowed to dry for 30 min in the bacteriological incubator. Disc of loaded hydrogel nanocomposite was cut using sterile cork bares and placed on the seeded media and incubated at 37°C for 24 h in bacteriological incubator. Finally, plate was observed for zone of inhibition. For negative control an unloaded (drug free) hydrogel nanocomposite was taken and the whole procedure was repeated.

3.7 Statistical analysis

All experiments were carried out at least thrice and data presented in the Figures and Tables have been shown along with appropriate error bars and standard deviations (SD), respectively.

4 Results and discussion

4.1 FTIR Spectra

The FTIR spectra of native PVA and prepared iron oxide impregnated hydrogels of a definite composition are depicted in Fig. 1a and b, respectively. The spectra (b) clearly reveals that the iron oxide impregnated gel presents combined spectral features of various functional groups of PVA and PMMA. Moreover, some characteristic bands of iron oxide are also present.

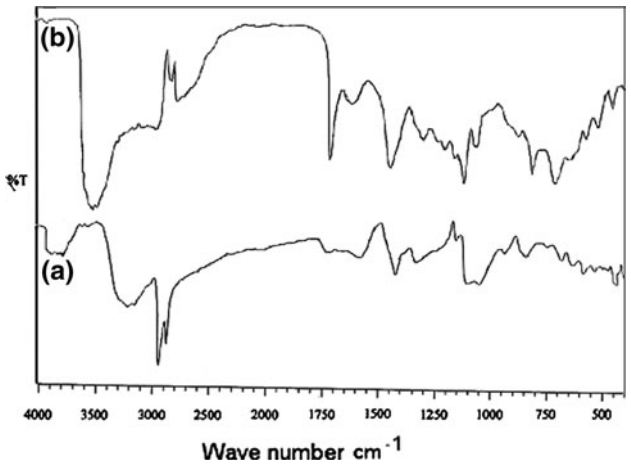

Fig. 1 FTIR spectra of **a** native PVA **b** iron oxide impregnated gel of definite composition: [PVA] = 2.0 g, [MMA] = 9.35 mM, [MBA] = 0.06 mM

Figure 1b represents the FTIR spectra of iron oxide impregnated PVA-g-PMMA gel film, as evident from the peaks observed at 3487 and 3526 cm^{-1} (typical of hydrogen bonded (bridged) O–H stretching vibrations of alcoholic OH and bound water), 2999 cm^{-1} (from C–H stretching of CH, CH_2 and CH_3 groups), 1157 and 1342 cm^{-1} (from twisting and wagging vibrations of methylene group, 1479 cm^{-1} (due to SP^3 C–H bending) 1111 cm^{-1} (due to C–O stretching of alcohol).

The characteristic peaks in Fig. 1b appearing at 1741, 1654 and 1214 cm^{-1} indicate the presence of stretching vibrations of the C=O ester group, C=C group and asymmetric coupled vibrations of C–C(=O)–O group of PMMA respectively, which also confirm the grafting of PMMA onto PVA.

The presence of iron oxide in the hydrogel is evident from the absorption bands appeared in the region between 450 and 480 cm^{-1} [18] and they may be assigned to Fe–O bonds of magnetite. The peaks at 521, 761 and 862 cm^{-1} [19] may also be due to the iron oxide lattice deformation and OH groups bound to the surface of the Fe_3O_4 nanoparticles. The spectra also show a peak at 581 cm^{-1}, characteristic of magnetite [20], and thus indicate the presence of magnetite particles in the polymer matrix.

4.2 Electron microscopy

The morphological features of the prepared impregnated gels have been investigated by SEM and TEM analysis of iron oxide particles as shown in Fig. 2a and b, respectively.

4.3 SEM

A close examination of the micrograph of iron oxide impregnated polymer matrix in Fig. 2a shows a

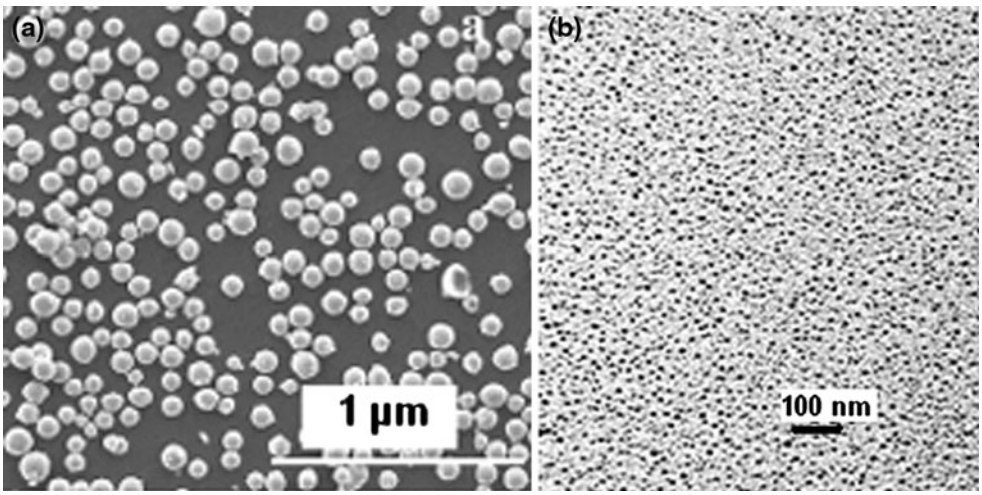

Fig. 2 SEM image of **a** iron oxide impregnated gel of definite composition: [PVA] = 2.0 g, [MMA] = 9.35 mM, [MBA] = 0.06 mM and **b** TEM image of iron oxide nanoparticles

homogeneous and even surface morphology. The impregnated iron oxide particles exhibit uniform size of nanometer dimensions.

4.4 TEM

In order to examine size of the iron oxide particles at nanoscale level TEM studies were performed. The TEM image shown in Fig. 2b reveals that an average size of the nanoparticles are about 9.52 nm and shape of the particles is also uniform.

4.5 XRD

In order to study the crystallographic nature of iron oxide nanoparticles and nanocomposite the XRD analysis was performed and respective XRD spectra are shown in Fig. 3a and b, respectively. The spectral patterns for iron oxide particles shown in Fig. 3a indicate the characteristic peaks at 18.2°, 30.0°, 35.4°, 43.1°, 53.3°, 57.0°. The interplaner distances using Bragg's equation were calculated to be 4.875, 2.979, 2.536, 2.099, 1.719, and 1.615 Å, respectively. The well defined X-ray diffraction patterns indicate the formation of highly crystalline iron oxide nanoparticles. The results also indicate that the prepared nanoparticles are pure magnetite with an inverse cubic spinal structure, which are identical to the standard XRD patterns of Fe_3O_4 [21]. X-ray diffraction patterns of the nanocomposite film shown in Fig. 3b indicate the characteristic peaks for poly (vinyl alcohol) and iron oxide at a 2θ values of 19.5 and 35.4 with their interplaner distances 4.554 and 2.536 Å, respectively. PVA is known to be of semi crystalline nature and shows a single broad peak at 19.5°. The XRD spectra shown in Fig. 3b depict an extra

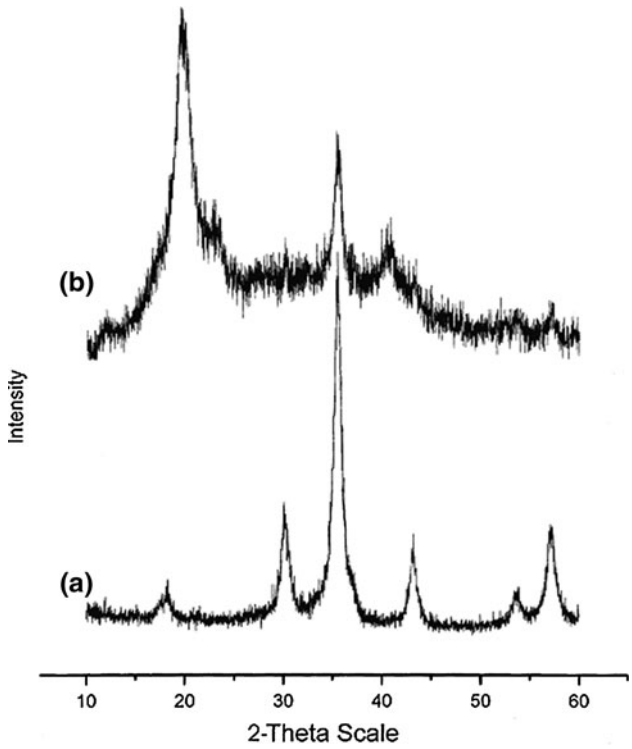

Fig. 3 XRD spectra of **a** iron oxide nanoparticles and **b** iron oxide impregnated gel of definite composition: [PVA] = 2.0 g, [MMA] = 9.35 mM, [MBA] = 0.06 mM

peak at 35.4°, thus, suggesting for characteristic peak of iron oxide. This obviously indicates the formation of iron oxide (magnetite) within the polymer matrix.

It is also clear from the Fig. 3a and b that the spectral intensity of the diffraction peaks of iron oxide in the composite is smaller as compared to that of the bulk

nanoparticles due to the reason that the concentration of nanoparticles is much smaller in the composite.

The mean grain size was calculated using Debye–Scherer formula [22] as shown in Eq. 6:

$$d = \frac{K\lambda}{\beta \cos \theta} \quad (6)$$

where d is mean grain size,k is the shape factor (0.9), β is broadening of the diffraction angle and λ is diffraction wavelength (1.54 Å).

From XRD spectra the crystallite size of iron oxide nanoparticles has been estimated to be 8.3 nm, which is in close agreement with the value of 9.52 nm calculated from TEM image.

The physical and mechanical properties of polymers are profoundly dependent on the degree of crystallinity. The percent (%) crystallinity of the iron oxide nanocomposites has been calculated by the following Eq. 7.

$$Xc\% = \frac{Ac}{Aa + Ac} \quad (7)$$

where Ac and Aa are the area of crystalline and amorphous phases, respectively [23]. The percent crystallinity of the nanocomposite was found to be ~58.3%. Since PVA is semi crystalline in nature, impregnation of iron oxide into the matrix increases its overall crystallinity whereas impregnated iron oxide nanoparticles loose their crystallinity as evident from the XRD spectra of pure iron oxide nanoparticles.

4.6 Magnetization studies

In order to explore the nature of magnetic behavior of the prepared nanocomposites, variation in magnetic moments of prepared iron oxide nanoparticles and their polymer composites was investigated as a function of varying magnetic field in the range −60 to 60 kOe. The results are shown in Fig. 4a–d which represent M-H plots for bulk nanoparticles (a and b) and nanocomposites (c and d), respectively.

Figure 4a and b show a typical magnetization (M) versus the applied magnetic field (H) plot. The saturation magnetization of the synthetic magnetic particles was found to be equal to 55 emu/g at 300 K, and 65 emu/g at 10 K, respectively. The values obtained are lower than the reported values of 92–100 emu/g for magnetite (Fe_3O_4) nanoparticles [24] and may be attributed to the fact that below a critical size, nanocrystalline magnetic particles may be single domain and show the unique phenomenon of superparamagnetism [25]. The magnetization curves also reveal that the value of Ms also increases with decreasing temperature and at both the temperatures i.e. 10 K and

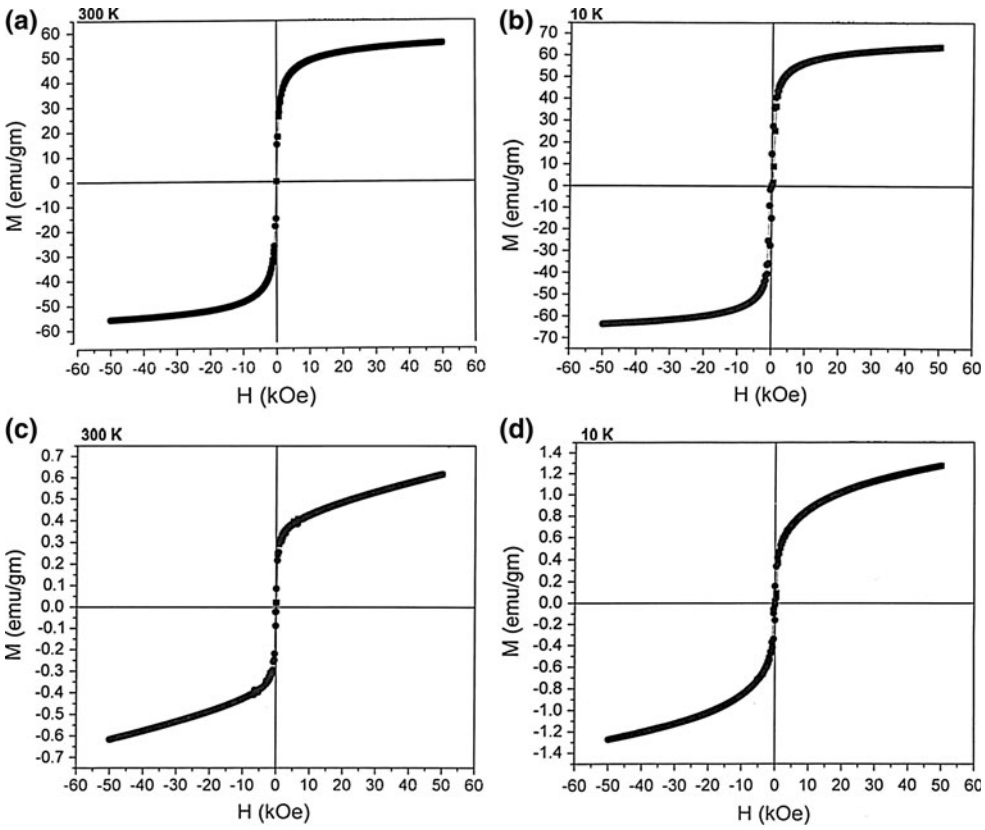

Fig. 4 Magnetization versus applied field curves **a** and **b** for magnetic nanoparticles, **c** and **d** for magnetic nanocomposites at 300 and 10 K respectively, of definite composition: [PVA] = 2.0 g, [MMA] = 9.35 mM, [MBA] = 0.06 mM

300 K, the superparamagnetism behavior of magnetic particles is maintained. The reason for this behavior may be that thermal effects, while not strong enough to overcome the forces between individual atoms, are strong enough to change the magnetization direction of the entire particle. This results in a random arrangement of magnetic directions among crystallites, thus giving a magnetic moment of zero.

Similar types of results are found when magnetite-polymer nanocomposites are investigated for M-H studies. The magnetization curves were constructed by measuring the magnetic moment under applied magnetic field varying in the range −60 to 60 kOe as shown in Fig. 4c and d. The measurements were carried out at 10 K and 300 K and the results clearly reveal that saturation magnetization is not attained even up to 60 kOe. The plots, however, indicate a zero remnant magnetization and coercivity thus suggesting that superparamagnetic behavior is still retained with the nanocomposite materials both at 300 and 10 K. The magnetization values, however, are significantly lower than the bulk magnetization values, which is quite obvious as diamagnetic nature of polymer matrix lowers the magnetization values. It is worth mentioning here that the observed remnance and zero coercivity clearly imply that in situ formation of magnetic nanoparticles within the polymer matrix produces much smaller sized particles which could also be a reason for lower magnetization values of the nanocomposite materials.

4.7 Mechanism of magnetic-sensitive drug release behavior

Magnetic field (MF) sensitive gels are unique materials in that they are mechanically soft and highly elastic and at the same time they exhibit a strong magnetic response [26]. The possible mechanism of the drug release from the ferrogel may be illustrated by the fact that the magnetic (fields) moments existing in ferrogel are randomly oriented. The ferrogel is subjected to zero magnetization, and the drug release displays a normal diffusion mode. While applying MF, the magnetic moments of the particles tend to align with the magnetic field and produce a bulk magnetic moment. This induces the magnetite particles within the ferrogel to aggregate together instantly, leading to a mechanical deformation in the ferrogel and encouraging the diffusion process, and as a consequence enhancing the release of drug with a MF than without it. It is also clear from all the effects that in the absence of MF the released amount of drug is lower and when the MF is applied there is a substantial increase in the released drug [27]. It is important to mention here that although in the present case direct current (DC) was used to produce magnetic field, however, since the drug containing nanocomposites were in constant and rapid motion, they were experiencing rapidly changing magnetic field and due to this fluctuation the magnetic nanoparticles produced friction within the matrix and result in loosening of the network chains of the nanocomposite.

4.8 Analysis of kinetic release data

In the present investigation the kinetic release data were analyzed in terms of exponent ‘n’ and diffusion constant ‘D’ and summarized in Table 1. It is clear from the Table 1 that for the PVA variation (1.5–3.0 g), except at the 2 g PVA the value of n in the anomalous region. The relaxation controlled nature of the release process at lower (1.5 g PVA) and higher (2.5 and 3 g PVA) amount of PVA could be attributed to the fact that at lower and higher content of PVA, the nanocomposite exhibits a lower degree of swelling because of lower hydrophilicity and high crosslink density of the nanocomposites, respectively.

On increasing the concentration of monomer MMA, in the feed mixture of the nanocomposite in the range 4.67–28.04 mM, the value of the release exponent n increases from 0.33 to 0.81 in the anomalous region. This clearly indicates a shift of mechanism from Fickian to anomalous type, i.e. from a diffusional controlled to relaxation controlled process. The observed results are due to their compact arrangement of chains which results in decreasing relaxation rates of network chains.

Due to the variation in the crosslinker (MBA) content of the nanocomposite, in the range 0.00–0.26 mM, the value of release exponent n varies from 0.44 to 0.62, thus, suggesting a shift of release mechanism from Fickian to anomalous type, i.e. from a diffusion controlled to relaxation controlled process. The observed shift is due to the reason that number of crosslinked chains in the network increases which restrains the mobility of macromolecular chains in the nanocomposite, thus rendering the release process to be relaxation controlled.

4.9 Release study of CFx

In the present paper the effect of various factors such as concentration of polymer, monomer, crosslinker and drug has been studied on the release rate. The effects of pH, magnetic field strength on drug release profile have also been investigated.

4.9.1 Effect of percent loading on released CFx

An important aspect in the use of hydrogel as drug vehicle is the effect of drug loading levels on the rate of drug release. As the drug concentration is an important factor in observed release rates the incorporation efficiency of the nanocomposites was evaluated for three different loading of CFx in the nanocomposites. Three drug solutions of CFx in

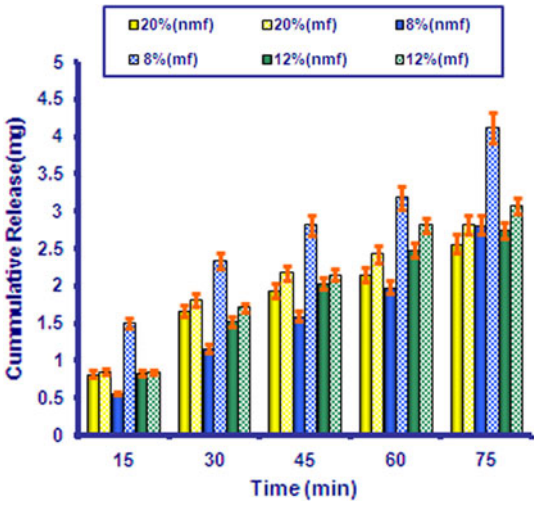

Fig. 5 Effect of percent loading on the release of CFx in the absence and presence of MF from the hydrogel nanocomposite of definite composition: [PVA] = 2.0 g, [MMA] = 9.35 mM, [MBA] = 0.06 mM

the concentration range 10–30 mg/mL were loaded and the obtained release results are displayed in Fig. 5 which reveals that the released amount of CFx decreases with increasing percent loading in the range 8–20%. The observed results may be attributed to the fact that with increasing % loading the pore size of hydrogel nanocomposites become smaller due to accumulation of drug molecules within the nanocomposites and this restrains the diffusion of release medium into the loaded hydrogel nanocomposites, which results in a lower release of CFx. Similar type of results have also been reported by other workers [28].

4.9.2 *Effect of PVA on released CFx*

In the present study the amount of PVA has been found to significantly affect the released amount of CFx. The effect of PVA on the release of CFx has been investigated by varying its concentration in the range 1.5–3 g in the feed mixture of the hydrogel. The results are shown in Fig. 6 which clearly indicates that the release of CFx increases up to 2.0 g of PVA while beyond it a fall in the released amount is observed. The above results can be explained on the basis of the hydrophilicity of the matrix which results in a greater degree of water sorption and hence a greater amount of CFx is released. However, on further increasing the concentration of PVA in the range 2.5–3.0 g the amount of released CFx decreases, because a further increase of PVA content in feed mixture of hydrogel nanocomposites enhances the crosslink density of the network which results in a lower degree of water sorption, which in turn leads to a lower release of entrapped CFx. Alternatively, beyond 2.5 g of PVA the enhanced interaction between drug and polymer may also lower the amount of released drug.

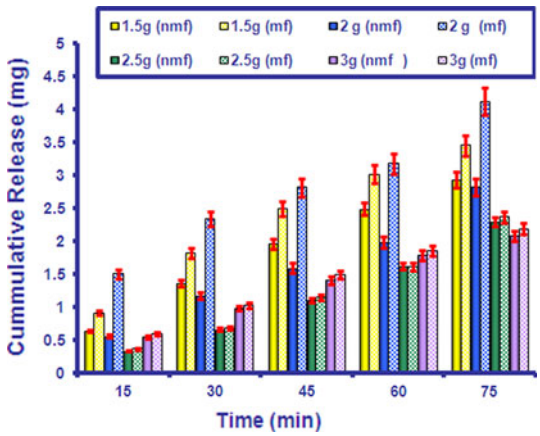

Fig. 6 Effect of varying amounts of PVA on the release of CFx in the absence and presence of MF from the hydrogel nanocomposite of definite composition: [MMA] = 9.35 mM, [MBA] = 0.06 mM

4.9.3 *Effect of MMA on released CFx*

The effect of monomer MMA on the release of CFx has been investigated by varying the monomer concentration in the range 4.67–28.04 mM. The release results are shown in Fig. 7 which clearly reveal that the release of CFx increases with increasing concentration from 4.67 to 9.35 mM while beyond it a fall in release of CFx is noticed, which clearly indicates that increasing molar concentration of MMA (4.67–9.35 mM) results in more longer chain lengths of PMMA, thereby increasing the mesh size of the free volumes available in between the macromolecular chains. However, at 18.69 mM concentration a fall in the released amount of CFx is noticed. This fall may be because of the reason that at higher concentration of MMA in feed mixture of the hydrogel nanocomposites, the polymeric matrices become largely crowded with PMMA chains and

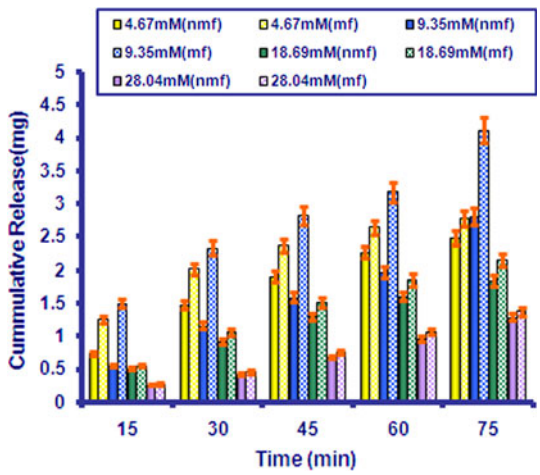

Fig. 7 Effect of varying amounts of MMA on the release of CFx in the absence and presence of MF from the hydrogel nanocomposite of definite composition: [PVA] = 2.0 g, [MBA] = 0.06 mM

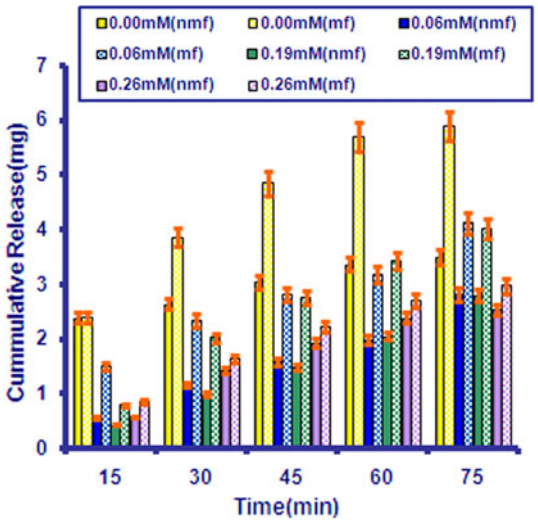

Fig. 8 Effect of varying amounts of MBA on the release of CFx in the absence and presence of MF from the hydrogel nanocomposite of definite composition: [PVA] = 2.0 g, [MMA] = 9.35 mM

this consequently increases the crosslink density to an appreciable extent and may not favor penetration of water molecules into the network thereby decreasing the release.

Another possible reason may be that with increase in PMMA content both the hydrophobicity and the interaction between the polymer chains and drug molecules increase which brings about a fall in released amount of drug.

4.9.4 Effect of MBA on released CFx

The effect of the degree of crosslinking on the drug release has been investigated in the range of 0.00–0.26 mM of MBA. The results are shown in Fig. 8 which clearly indicates that on increasing the concentration of MBA in the studied range the release of CFx is appreciably reduced. The observed results are quite expected because on increasing the MBA content in the hydrogel, the number of crosslink points in the hydrogel increases, which enhances the compactness of the macromolecular network which consequently reduces the free volume accessible to the penetrant water molecules. Similar types of results have also been published elsewhere [29].

4.9.5 Effect of MF variation on released CFx

To evaluate the effect of MF on the release of CFx, the MF has been varied in the range of 75–250 G. The results are depicted in Fig. 9 which reveals that the released amount of CFx decreases with increasing strength of magnetic field. When we increase the magnetic field strength current will also increase which increases the heat of the system and decreases the magnetic field strength. This explains why the released amount of CFx decreases with increasing

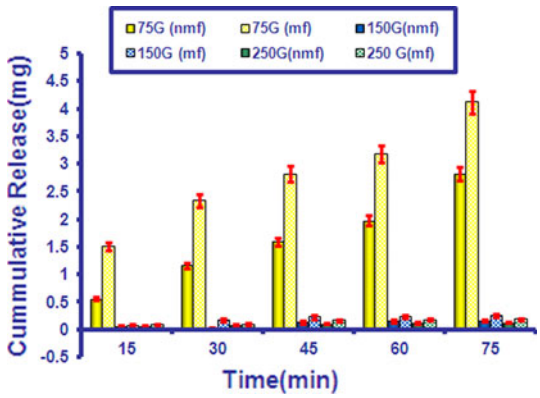

Fig. 9 Effect of magnetic field on the release of CFx in the absence and presence of MF from the nanocomposite of definite composition: [PVA] = 2.0 g, [MMA] = 9.35 mM, [MBA] = 0.06 mM

magnetic field strength. Similar type of results has also been reported by other workers [30].

4.9.6 Effect of pH on release of CFx

In the present investigation the effect of pH has been investigated in the pH range 1.8–8.6 which are identical to those found in the GI tract. The results are depicted in Fig. 10 which show that the release of CFx is found more at 1.8 (acidic) and 8.6 (basic) medium than 7.4 pH. The release of CFx decreases with increasing pH of the medium and attains lowest release at neutral pH. However, after increasing the pH in the alkaline range the release of CFx again increases. The results may be explained as below:

According to the Flory's theory of swelling of network the release is caused by osmotic pressure difference

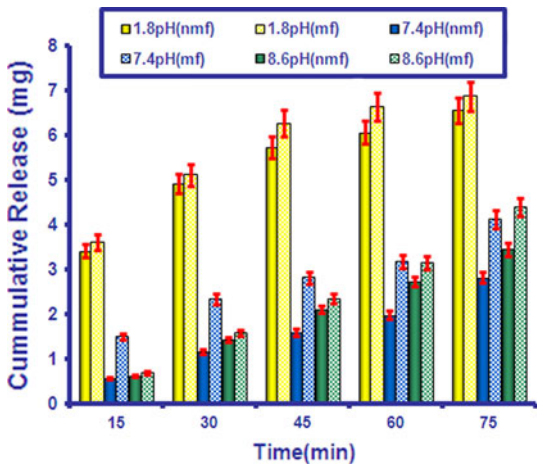

Fig. 10 Effect of pH on the release of CFx in the absence and presence of MF from the hydrogel nanocomposite of definite composition: [PVA] = 2.0 g, [MMA] = 9.35 mM, [MBA] = 0.06 mM

$\Pi_{in} - \Pi_{out}$ at the inside and outside of the hydrogel nanocomposite [31]. This difference results in an ion osmotic pressure (Π_{ion}) given by the following eq.

$$\Pi_{ion} = RT \sum \left(C_i^g - C_i^s\right) \quad \text{.....} \quad (8)$$

where C_i^g and C_i^s represent the mobile ion concentrations inside and outside the nanocomposite, respectively. The osmotic pressure (Π) results from a net difference in concentration of mobile ions between the interior of the nanocomposite at external medium. Increasing ionic concentration difference results in an enhanced swelling of the polymer which, in turn, will bring about an increase in the amount of released drug.

In the present work, however, the hydrogel is nonionic in nature but CFx may exist in solution in diprotonated (H_2cipxq), monoprotonated (Hcipx), zwitterionic (Hcipx $\pm$) and anionic (cipx$\bar{y}$) forms [32]. The results can be explained by the fact that the CFx (amphoteric in nature) undergoes partial hydrolysis, and consequently produce cationic charged centers. When the pH is 1.8, ionic concentration within the nanocomposite becomes quite great due to the NH_2^+ ion of CFx, which increases the difference in ionic concentration between the external and internal medium. Therefore, the degree of water sorption increases which obviously enhances the extent of CFx release.

Similar type of results have also been obtained in alkali medium.The results can be explained by fact that the COOH groups undergo a partial hydrolysis to produce anionic groups COO^-. Now these ions cause repulsive forces and thus macromolecular chains undergo a fast relaxation which facilitates the penetration of water molecules into the loaded nanocomposite. As a consequence the amount of released CFx increases.

4.10 Drug activity

4.10.1 UV spectral study

The chemical activity of the drug was investigated by recording the UV spectra of native CFx in solution and released CFx in the range 240–380 nm as shown in Fig. 11. On comparing the spectra of pure and released drug solutions it is revealed that the spectra are almost identical, and thus suggests that no significant change in chemical and bioactivity of the drug may have occurred during loading and release of the drug. Similar type of comparison to assess the chemical and bioactivity of drug has also been reported elsewhere [33].

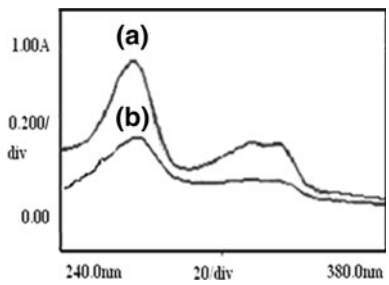

Fig. 11 UV spectra showing the chemical stability of CFx in its pure solution (**a**) and released media (**b**)

4.10.2 Antibacterial activity

Antibacterial activity of CFx has been demonstrated in Fig. 12 which exhibits a clear zone around loaded nanocomposite disk where the growth has been inhibited. This zone is known as zone of inhibition. Formation of inhibition zone shows that CFx can easily diffuse into agar media from loaded nanocomposites and its antibacterial activity remains unchanged after loading into the nanocomposite. It was noticed that no inhibition zone was formed with unloaded nanocomposites which also favors antibacterial activity of CFx.

5 Conclusions

Magnetically guided drug delivery has emerged as one of the most promising strategies to treat complex diseases like cancers. This approach results in delivering the required amount of drug to the desired location thus minimizing the adverse side effects normally experienced by the normal tissues. In order to achieve the optimum benefits, it is essential to have a superparamagnetic matrix (or carrier)

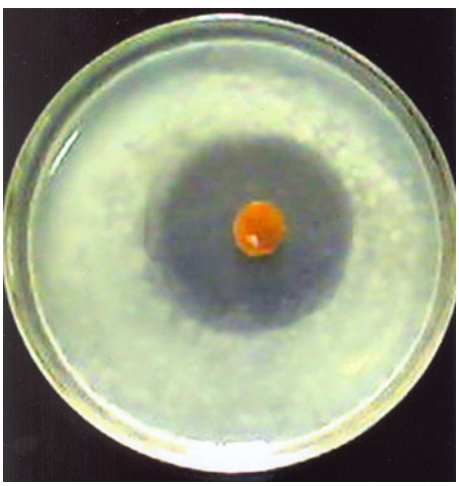

Fig. 12 Photograph depicting the evidence of antibacterial activity of released CFx from the hydrogel nanocomposite of definite composition: [PVA] = 2.0 g, [MMA] = 9.35 mM, [MBA] = 0.06 mM

of biocompatible nature. In this way, the prepared nanocomposite matrix in the present investigation could be an excellent material to achieve the goal.

Redox polymerized methyl methacrylate in the presence of polyvinyl alcohol results in a polymer matrix of adequate hydrophilicity. The matrix functions as an ideal medium for homogenous in situ precipitation of magnetite nanoparticles which is further confirmed by FTIR.

The scanning electron microscopy (SEM) suggests that the surface of the iron oxide impregnated polymer matrix has a homogeneous and even morphology. The nanocomposite contains magnetite particles having nanometer dimensions. The transmission electron microscopy (TEM) of the nanoparticles suggests for an average size of 9.52 nm of the magnetite nanoparticles.

The XRD analysis of bulk magnetite nanoparticles and nanocomposite reveal that the former are more crystalline in nature and their incorporation into the polymer matrix brings about a fall in the overall crystallinity. The size of the nanoparticles calculated by Debye–Scherer equation has been found to be 8.3 nm which agrees well with that estimated by TEM (9.52 nm).

When the prepared iron oxide nanoparticles and nanocomposites are put under varying magnetic field, magnetic moment is developed which increases with increasing field strength. It is also observed that the magnetic moment of bulk nanoparticles is much greater than nanocomposite matrices, and both the bulk nanoparticles and nanocomposites exhibit superparamagnetic behavior.

The release of the drug CFx is accelerated in the presence of magnetic field and follows anomalous behavior with higher and lower amounts of PVA while with increasing concentration of MMA and MBA the release mechanism shifts from Fickian to anomalous. The release of the drug is found to decrease with increasing percent loading. It is also noticed that the released amount of drug increases with increasing amount of PVA in the range 1.5–2.0 g while a fall is noticed when the amount of PVA exceeds 2.0 g. In the case of MMA the extent of release increases with increasing concentration of MMA up to 9.35 mM, while beyond it a decrease in release of drug is noticed. However, with increasing crosslinker MBA (4.67–28.04 mM) the extent of release constantly decreases.

The amount of released CFx also decreases with increasing intensity of magnetic field. The pH of the release medium significantly affects the release profile and it is noticed that at both the acidic (pH 1.8) and alkaline (pH 8.6) the release is greater than that at pH 7.4. It is also found that at pH 7.4 the drug seems to be stable. The loaded nanocomposite film also exhibits antibacterial behavior.

Thus, the prepared magnetite–polymer matrices with desirable properties seem promising to serve as a carrier for control and targeted drug delivery applications.

References

1. Ciofani G, Riggio C, Raffa VA, Menciassi A, Cuschieri A. A bi-modal approach against cancer: magnetic alginate nanoparticles for combined chemotherapy and hyperthermia. Med Hypotheses. 2009;73:80–2.
2. Mahmoudi M, Simchi A, Milani AS, Stroeve P. Cell toxicity of superparamagnetic iron oxide nanoparticles. J Colloid Interface Sci. 2009;336:510–8.
3. Hu SH, Liu TY, Tsai CH, Chen SY. Preparation and characterization of magnetic ferroscaffolds for tissue engineering. J Magn Magn Mater. 2007;310:2871–3.
4. Jain KK. Targeted Drug Delivery for Cancer. Tech Cancer Res Treat. 2005;4(4):311–3.
5. Lubbe AS, Alexiou C, Bergemann C. Clinical Applications of Magnetic Drug Targeting. J Surg Res. 2001;95:200–6.
6. Jain TK, Richey J, Strand M, Leslie-Pelecky DL, Flask CA, Labhasetwar V. Magnetic nanoparticles with dual functional properties: drug delivery and magnetic resonance imaging. Biomaterials. 2008;29:4012–21.
7. Ge Y, Zhang Y, guang Xia J, Ma M, He S, Nie F, Gu N. Effect of surface charge and agglomerate degree of magnetic iron oxide nanoparticles on KB cellular uptake in vitro. Colloids Surf B. 2009;73:294–301.
8. Maity D, Agarwal DC. Synthesis of iron oxide nanoparticles under oxidizing environment and their stabilization in aqueous and non-aqueous media. J Magn Magn Mater. 2007;308:46–55.
9. Bajpai AK, Bajpai J, Soni SN. Preparation and characterization of electrically conductive composites of poly (vinyl alcohol)-g-poly (acrylic acid) hydrogels impregnated with polyaniline (PANI). eXPRESS Polym Lett. 2008;2(1):26–39.
10. Singh MK, Shokuhfar T, de Almeida Gracio JJ, Mendes de Sousa AC, Da Fonte Fereira JM, Garmestani H, Ahzi S. Hydroxyapatite modified with carbon nanotube-reinforced Poly(methyl methacrylate): a novel nanocomposite material for biomedical applications. Adv Funct Mater. 2008;9999:1–7.
11. Zhao H, Le Y, Liu H, Hu T, Shen Z, Yun J, Chen JF. Preparation of microsized spherical aggregates of ultrafine ciprofloxacin particles for dry powder inhalation (DPI). Powder Technol. 2009;194:81–6.
12. Mockovciakova A, Orolinova Z, Matik M, Hudec P, Kmecova E. Iron oxide contribution to the modification of natural zeolite. Acta montanistica Slovaca. 2006;11:353–7.
13. Bajpai AK, Kankane S. Preparation and characterization of macroporous poly (2-hydroxyethyl methacrylate)-based biomaterials: Water sorption property and in vitro blood compatibility. J Appl Polym Sci. 2007;104:1559–71.
14. Bajpai AK, Singh R. Study of biomineralization of poly (vinyl alcohol)-based scaffolds using an alternate soaking approach. Polym Int. 2007;56:557–68.
15. Tang JG, Hu K, Liu HY, Gao D, Wu RJ. Synthesis of 10 nanometric copper clusters in a polymer matrix by a solution-reduction synthesis (SRS). J Appl Polym Sci. 2000;76:1857–64.
16. McNeild ME, Graham NB. Properties controlling the diffusion and release of water-soluble solutes from poly(ethylene oxide) hydrogels. 4. Extended constant rate release from partly-coated spheres. J Biomater Sci Polym Ed. 1996;7(11):953–63.

17. Bauer AW, Kirby WMM, Sherris JC, Truck M. Antibiotic susceptibility testing by a standardized single disk method. Am J Clin Pathol. 1966;45:493–6.
18. Zhong ZY, Prozorov T, Felner I, Gedanken A. Sonochemical synthesis and characterization of iron oxide coated on submicrosphrical alumina: A direct observation of interaction between iron oxide and alumina. J Phys Chem B. 1999;103:947–56.
19. Kryszewski M, Jeszka JK. Nanostuructured conducting polymer composites-superparamagnetic particles in conducting polymers. Synth Mater. 1998;94:99–104.
20. Schwartzman V, Cornell RM. Iron oxide in the laboratory: preparation and Characterization. 2nd ed. New York: Wiley; 2000.
21. Mandal M, Kundu S, Ghosh SK, Panigrahi S, Sahu TK, Yusuf SM, Pal T. Magnetite nanoparticles with tunable gold or silver shell. J Colloid Interface Sci. 2005;286:187–94.
22. Bajpai AK, Bundela H. Designing of hydroxyapatite-gelatin based porous matrix as bone substitute: Correlation with biocompatibility aspects. eXPRESS Polym Lett. 2008;2:201–13.
23. Gupta B, Kothari VK. Manufactured Fiber Technology. London: Chapman & Hall; 1997. p. 225.
24. Morales M, Jain TK, Labhasetwar V. Magnetic studies of iron oxide nanoparticles coated with oleic acid and pluronic® block copolymer. J Appl Phys. 2005;97:10Q905 (1-3).
25. Chia CH, Zakaria S, Ahamd S, Abdullah M, Jani SM. Preparation of magnetic paper from kenaf: lumen loading and in situ synthesis method. Am J Appl Sci. 2006;3:1750–4.
26. Szaba D, Czako-Nagy I, Zrinyi M, Vertws A. Magnetic and mossbauer studies of magnetite loaded polyvinyl alcohol hydrogels. J Colloid Interface Sci. 2000;221:166–72.
27. Rana S, Gallo A, Srivastava RS, Mishra RD. On the suitability of nanocrystalline ferrites as a magnetic carrier for drug delivery: functionalization, conjugation and drug release kinetics. Acta Biomater. 2007;3:233–42.
28. Bajpai AK, Mishra A. Carboxymethyl cellulose (CMC) based semi-IPNs as carriers for controlled release of ciprofloxacin: an in vitro dynamic study. J Mater Sci: Mater Med. 2008;19:2121–30.
29. Bajpai AK. Adsorption of a blood protein on to hydrophilic sponges based on poly(2-hydroxyethyl methacrylate). J Mater Sci: Mater Med. 2004;15:583–92.
30. Bajpai AK, Choubey J. Investigation on magnetically controlled delivery of doxorubicin from superparamagnetic nanocarriers of gelatin crosslinked with genipin. J Mater Sci: Mater Med. 2010;21:1573–86.
31. Flory PJ. Principles of Polymer Chemistry. Ithaca: Cornell University Press; 1953.
32. Djurdjevic P, Stankov MJ, Odovic J. Study of solution equilibria between iron(III) ion and ciprofloxacin in pure nitrate ionic medium and micellar medium. Polyhedron. 2000;19:1085–96.
33. Wang LF, Chen WB, Chen YB, Lu SC. Effects of the preparation methods of hydroxypropyl methylcellulose/polyacrylic acid blended films on drug release. J Biomater Sci: Polym Ed. 2003; 14(1):27–44.